ELSEVIER

Journal of Alloys and Compounds 434–435 (2007) 106–109

Journal of ALLOYS AND COMPOUNDS

www.elsevier.com/locate/jallcom

Microstructural investigation of a deformed $Ti_{66.1}Cu_8Ni_{4.8}Sn_{7.2}Nb_{13.9}$ nanostructure–dendrite composite

K.B. Kim [a,*], J. Das [b], F. Baier [c], J. Eckert [b]

[a] *Department of Advanced Materials Engineering, Sejong University, 98 Gunja-dong, Gwangjin-gu, Seoul 143-747, Seoul, Korea*

[b] *Leibniz-Institut für Festkörper- und Werkstoffforschung Dresden, Helmholtzstr. 20, D-01069 Dresden, Germany*

[c] *FG Physikalische Metallkunde, FB 11 Material- und Geowissenschaften, Technische Universität Darmstadt, Petersenstraße 23, D-64287 Darmstadt, Germany*

Available online 29 September 2006

Abstract

Investigation of the microstructure of a compressed $Ti_{66.1}Cu_8Ni_{4.8}Sn_{7.2}Nb_{13.9}$ nanostructure–dendrite composite reveals that the deformed bcc β-Ti dendrites form a stepped morphology at the interfaces between the individual dendrites and the nanostructured matrix of hcp α-Ti and bct Ti_2Cu phases. Furthermore, there is a unique stained contrast during the propagation and the interaction of the shear bands in the dendrites indicating a local structural change near to the apex of the shear bands in the dendrite. In contrast, the shear bands pass through coherent grain boundaries between the hcp α-Ti and the bct Ti_2Cu phases of the nanostructured matrix.

Keywords: Nanostructured materials; Mechanical properties; Transmission electron microscopy

1. Introduction

A series of Ti- and Zr-based BMG in situ composites with nano-scale precipitates [1,2] or ductile dendrites [3,4] have been successfully fabricated with a significant improvement of the macroscopic ductility. Furthermore, so-called "ductile" BMGs have been also developed by fine-tuning the composition of good glass-forming Zr- [4], Pt- [5], Cu- [6] and CuZr-based [7–9] alloys.

Along the line to enhance the macroscopic ductility, nanostructure–dendrite composites have been also successfully developed in a series of Ti- [10–13] and Zr-based [14,15] multicomponent alloys with promising mechanical properties, i.e. high strength of more than 2 GPa and large ductility of more than 15% at room temperature. Recently, a systematic microstructural investigation revealed that work hardening occurs by the formation of slip bands in the dendrites of a $Ti_{62}Nb_8Ni_{12}Cu_{14}Sn_4$ nanostructure–dendrite composite at the initial stage of the plastic deformation (5% strain) [16]. With increasing deformation up to 13.5% the formation of shear bands, which are initiated at the interfaces between the dendrites and the nanostructured matrix, was observed [16]. These results suggest that the work hardened dendrites can resist the propagation of the shear bands during deformation.

However, the details of the interactions of the shear bands in the nanostructure–dendrite composite during deformation are still not fully understood. In this letter, the propagation and intersection of shear bands in correlation with the microstructure of the dendrites and the nanostructured matrix of the $Ti_{66.1}Cu_8Ni_{4.8}Sn_{7.2}Nb_{13.9}$ nanostructure–dendrite composite are investigated in detail by transmission electron microscopy (TEM) after an overall deformation of 25%.

2. Experimental

The details of the experimental procedures used for casting the specimens were described in a previous report [10,11]. The investigated samples with 4 mm diameter and 8 mm length were deformed up to a total strain of 25% by compression testing at room temperature using an Instron 8562 device. After deformation, the cross-sectional area of the deformed samples was sliced by precision cutting. Phase analysis was performed using X-ray diffraction (XRD, Siemens D500) with Cu Kα radiation. Scanning electron microscopy (SEM, Zeiss 962) was employed to investigate the surface morphology of the deformed samples. Detailed microstructural investigations were done by transmission

* Corresponding author at: Department of Advanced Materials Engineering, Sejong University, Korea. Tel.: +82 2 3408 3690; fax: +82 2 3408 3664.
E-mail address: kbkim@sejong.ac.kr (K.B. Kim).

0925-8388/$ – see front matter © 2006 Elsevier B.V. All rights reserved.
doi:10.1016/j.jallcom.2006.08.133

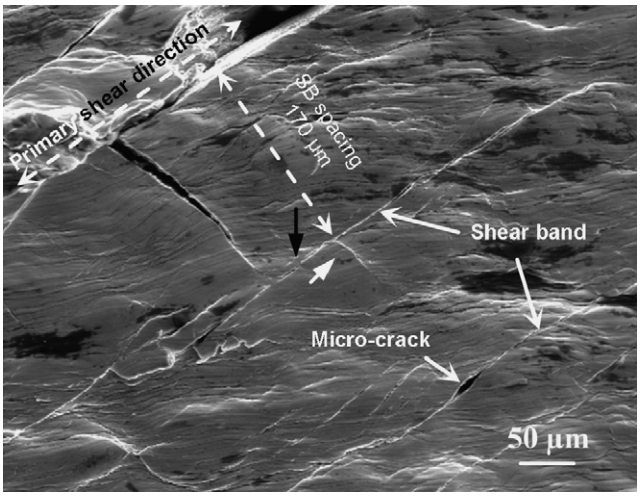

Fig. 1. SEM secondary electron image for the deformed $Ti_{66.1}Cu_8Ni_{4.8}Sn_{7.2}Nb_{13.9}$ alloy. The black and white arrows indicate the shear bands.

electron microscopy (TEM, Philips CM 20) coupled with energy-dispersive X-ray analysis (EDX, Noran). The TEM samples were prepared by the conventional method of slicing and grinding, followed by dimpling and finally ion-milling.

3. Results and discussion

Fig. 1 shows a SEM secondary electron image obtained from the surface of the deformed $Ti_{66.1}Cu_8Ni_{4.8}Sn_{7.2}Nb_{13.9}$ alloy. Homogeneously distributed shear bands in the surface are visible indicating that there was no significant localization of the shear bands. The primary and secondary shear bands occur perpendicularly, as marked by black and white arrows, respectively.

Fig. 2(a) shows a TEM bright-field image and the corresponding selected area diffraction pattern of the deformed $Ti_{66.1}Cu_8Ni_{4.8}Sn_{7.2}Nb_{13.9}$ alloy. The microstructure of the dendrites exhibits several shear bands, which are homogeneously distributed throughout the specimen. The distance between the shear bands is approximately 150–250 nm. Furthermore, shear bands also formed perpendicularly, as marked by the black arrows in Fig. 2. One can observe the typical contrast caused by the strain of the shear bands in the dendrites. The inset in Fig. 2(a) shows the corresponding selected area diffraction (SAD) pattern of the dendrites. The SAD pattern was identified as the [1 1 1] zone axis of the bcc β-Ti dendrites. The morphology of the interface between the dendrites and the nanostructured matrix is stepped along the direction parallel to the direction of the shear band. The distance between the steps in the interfaces of 80–200 nm is similar to that of the shear bands. This indicates that the shear bands penetrate the interfaces between the dendrites and the nanostructured matrix, and suggests that the extra area of the interface due to the formation of the stepped interfaces is produced in order to accommodate the shear strains [17]. Furthermore, the distance between the steps in the interfaces agrees well with the distance between the primary shear bands in the dendrites and with the width of the granular grains in the nanostructured matrix. This indicates that the primary shear bands, that are generated at the interface between the dendrites and nanostructured matrix, pass through the interfaces by releasing the shear strains and by this contribute to the overall ductility of the sample [17].

A more detailed TEM dark-field image of the shear bands in a dendrite taken at higher magnification is shown in Fig. 2(b). The stained contrast indicates that the dendrites are strained by the propagation and intersection of the shear bands. In particular, a triangle-shaped contrast is often observed at the edge of the interaction region between the shear bands (marked by a single black-colored star in Fig. 2(b)). The stained contrast is obtained at the intersection areas throughout the dendrites, suggesting that local structural changes may occur during the intersection. This is similar to pressure- and shock-induced solid state amorphization as it has been reported for densified porous silicon [18] and boron carbide [19]. Therefore, the

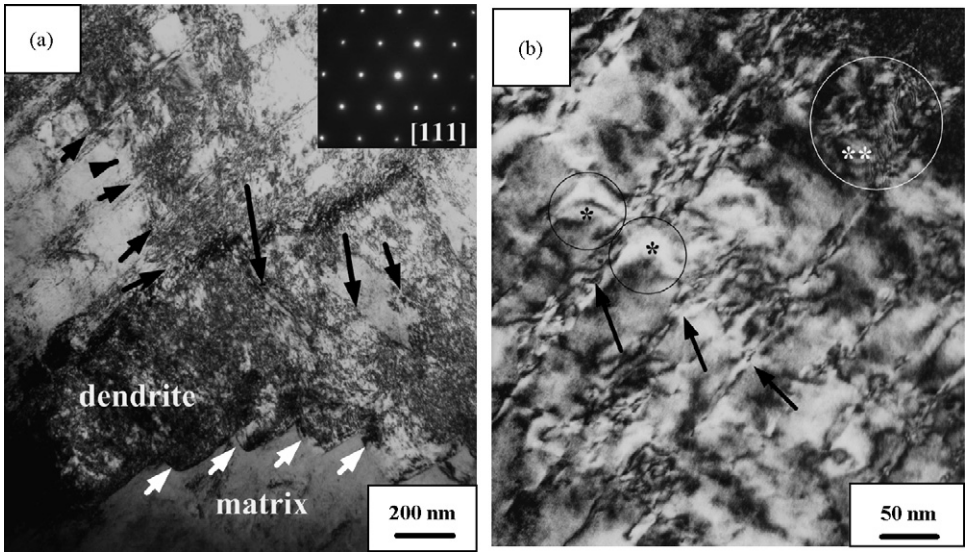

Fig. 2. TEM bright- and dark-field images (a and b) and the corresponding selected area diffraction pattern (inset in part (a)) of the deformed $Ti_{66.1}Cu_8Ni_{4.8}Sn_{7.2}Nb_{13.9}$ alloy. The single black-colored star and the two white-colored stars indicate the areas of the triangle contrast and the moiré fringes, respectively.

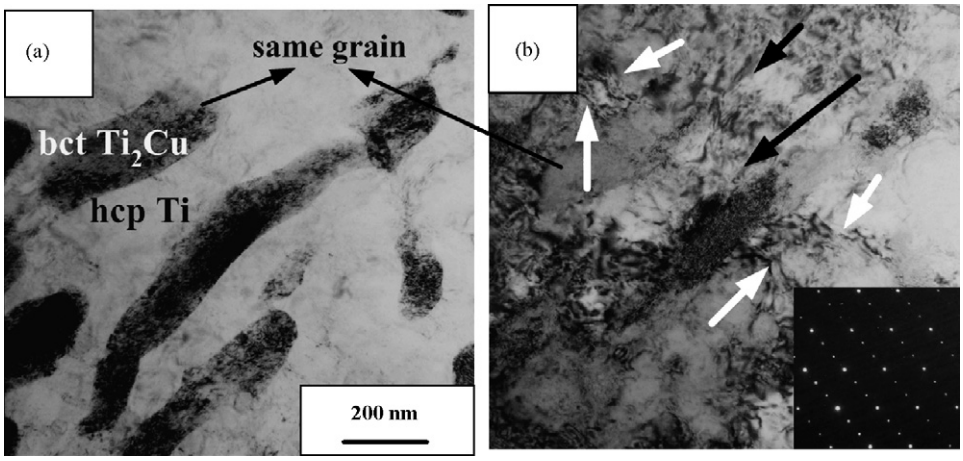

Fig. 3. TEM bright-field images (a and b) and the corresponding selected area diffraction patterns (inset in part (b)) for the nanostructued matrix of the deformed $Ti_{66.1}Cu_8Ni_{4.8}Sn_{7.2}Nb_{13.9}$ alloy. The bright-field images were obtained from the same region of the sample with different tilting angle of 9°. The shear bands are marked by arrows.

occurrence of the local amorphization is very feasible at the intersection sites of the shear bands in the dendrites [20]. Besides, one can also observe moiré fringes at the edge of the interaction regions between the primary and secondary shear bands (marked by two white-colored stars in Fig. 2(b)). This suggests that the local structure of the dendrite changes by translation and rotation without forming interfaces [21].

Fig. 3 shows TEM bright-field images (a and b) and a corresponding selected area diffraction pattern of the nanostructued matrix of the deformed $Ti_{66.1}Cu_8Ni_{4.8}Sn_{7.2}Nb_{13.9}$ alloy (inset in Fig. 3(b)). The bright-field image (a) exhibits two types of contrast in the nanostructured matrix. Most of the grains are granular with 100–160 nm in width and 200–800 nm in length along the direction of the shear bands, marked by black arrows. The bright-field image in Fig. 3(b) was obtained from the same area of the nanostructured matrix shown in Fig. 3(a) after tilting the sample by 9°. This bright-field image reveals that the shear bands pass through the boundaries of the granular grains parallel to the direction of the shear bands. Furthermore, moiré fringes are frequently observed at the grain boundaries indicating the structural coherency between the phases in the matrix [17]. On the other hand, the shear bands with a perpendicular direction, marked by white arrows, are arrested by the grains, thus forming highly strained regions. The coherency of the grain boundaries between the two matrix phases may retard the formation of cracks by generating shear bands with a perpendicular direction [22]. This may occur due to the sandwiched nano-scale microstructure, i.e. 100–160 nm large arrays of granular grains in the matrix, consisting of the hcp α-Ti and bct Ti_2Cu phases, similar as in multilayered structures. Therefore, the propagation of the secondary shear bands, arrested in the sandwiched nano-scale microstructures, can contribute to the overall strength of the samples. The selected area diffraction pattern (inset in Fig. 3(b)) corresponds to the combination of the [1 −1 0 1] zone axis from the hcp α-Ti phase and the [1 0 0] zone axis of the bct Ti_2Cu phase. The diffraction peaks are overlapping between the two phases indicating the presence of coherent grain boundaries between the hcp α-Ti and bct Ti_2Cu phases [22].

4. Summary

A strong interaction of the shear bands is observed in the dendrites of the $Ti_{66.1}Cu_8Ni_{4.8}Sn_{7.2}Nb_{13.9}$ nanostructure–dendrite composite after deformation up to 25%. The shear bands form a stepped morphology at the interfaces between the dendrites and the nanostructured matrix, indicating the penetration of the shear bands through the interfaces between the dendrites and the matrix. A detailed analysis reveals that a stained contrast in the dendrites occurs locally near to the apex of the shear bands. This suggests that the propagation of the shear bands can be retarded by releasing the accumulated shear strains by both the generation of the extra interface area, formed by the stepped morphology, and the local structural changes of the material. The shear bands, initiated from the interfaces between the dendrites and the nanostructured matrix pass through the coherent grain boundaries of the nano-scale granular grains in the matrix during deformation. In contrast, the shear bands with a perpendicular direction in the nanostructured matrix are arrested in the sandwiched nano-scale microstructure. Consequently, the propagation of these shear bands in the nanostructured matrix can contribute to the overall strength of the sample.

Acknowledgements

The authors thank G. He, G. Miehe, C. Müller, R. Theissmann, W. Xu, P. Yu and Z.F. Zhang for technical assistance and stimulating discussions, and U. Kunz for TEM sample preparation. Funding by the EU within the framework of the Research Training Network on ductile bulk metallic glass composites (MRTN-CT-2003-504692) is gratefully acknowledged.

References

[1] G. He, W. Löser, J. Eckert, L. Schultz, J. Mater. Res. 17 (2002) 3015.
[2] Y.C. Kim, J.H. Na, J.M. Park, D.H. Kim, J.K. Lee, W.T. Kim, Appl. Phys. Lett. 83 (2003) 3093.
[3] C.C. Hays, C.P. Kim, W.L. Johnson, Phys. Rev. Lett. 84 (2000) 2901.

[4] U. Kühn, J. Eckert, N. Mattern, L. Schultz, Appl. Phys. Lett. 80 (2002) 2478.
[5] L.Q. Xing, Y. Li, K.T. Ramesh, J. Li, T.C. Hufnagel, Phys. Rev. B 64 (2001) 180201.
[6] J. Schroers, W.L. Johnson, Phys. Rev. Lett. 93 (2004) 255506.
[7] A. Inoue, W. Zhang, T. Zhang, K. Kurosaka, Mater. Trans. JIM 42 (2001) 1149.
[8] J. Das, M.B. Tang, K.B. Kim, R. Theissmann, F. Baier, W.H. Wang, J. Eckert, Phys. Rev. Lett. 94 (2005) 205501.
[9] Q. Cao, J. Li, Y. Zhou, J. Jiang, Appl. Phys. Lett. 86 (2005) 081913.
[10] G. He, J. Eckert, W. Löser, L. Schultz, Nat. Mater. 2 (2003) 33.
[11] G. He, J. Eckert, W. Löser, M. Hagiwara, Acta Mater. 52 (2004) 3035.
[12] D.V. Louzguine, H. Kato, A. Inoue, J. Alloys Compd. 384 (2004) L1.
[13] D.V. Louzguine, H. Kato, A. Inoue, Philos. Mag. Lett. 84 (2004) 359.
[14] J. Das, W. Löser, U. Kühn, J. Eckert, S.K. Roy, L. Schultz, Appl. Phys. Lett. 82 (2003) 4690.
[15] J. Das, A. Güth, H.-J. Klauß, C. Mickel, W. Löser, J. Eckert, S.K. Roy, L. Schultz, Scripta Mater. 49 (2003) 1189.
[16] H. Zhang, X.F. Pan, Z.F. Zhang, J. Das, K.B. Kim, C. Müller, F. Baier, M. Kusy, A. Gebert, G. He, J. Eckert, Z. Metallkd. 96 (2005) 675.
[17] K.B. Kim, J. Das, F. Baier, J. Eckert, Appl. Phys. Lett. 86 (2005) 171909.
[18] S.K. Deb, M. Wilding, M. Somayazulu, P.F. McMillan, Nature 414 (2001) 528.
[19] M. Chen, J.W. McCauley, K.J. Hemker, Science 299 (2003) 1563.
[20] K.B. Kim, J. Das, F. Baier, J. Eckert, Appl. Phys. Lett. 86 (2005) 201909.
[21] Z.F. Zhang, G. He, H. Zhang, J. Eckert, Scripta Mater. 52 (2005) 945.
[22] K.B. Kim, J. Das, F. Baier, J. Eckert, Phys. Status Solidi A 202 (2005) 2405.